

Impact of spatial curvature on quantum Otto engines

S. Kourkinejat,^{1,*} A. Mahdifar,^{1,2,†} and E. Amooghorban^{3,4,‡}

¹*Physics Department, University of Isfahan, Hezar Jerib St. Isfahan, 81764-73441, Iran.*

²*Quantum Optics Group, Department of Physics, University of Isfahan, Hezar Jerib St. Isfahan, 81746-73441, Isfahan, Iran.*

³*Department of Physics, Faculty of Science, Shahrekord University P. O. Box 115, Shahrekord, Iran*

⁴*Nanotechnology Research Center, Shahrekord University, 8818634141, Shahrekord, Iran*

(Dated: October 30, 2024)

In this paper, we consider a quantum Otto cycle with a quantum harmonic oscillator on a circle as its working substance. Since the eigen-energies of this oscillator depend on the curvature of the circle, this model, as an analog model, enables us to investigate the curvature effects of the physical space on properties of quantum heat engines. We assume that two classical hot and cold thermal baths are located at places with different curvatures. We calculate the curvature-dependent work and heat in our Otto cycle with a particular emphasis on how curvature affects its thermal efficiency. By changing the curvature difference between the bath's locations, we find that the efficiency of our heat engine can exceed the Carnot efficiency limit.

I. INTRODUCTION

Einstein's theory of general relativity indicates that massive objects change the geometric nature, and thus, the curvature of the surrounding space-time, leading to some curvature-dependent effects [1, 2]. Furthermore, the equivalence principle provides a clear insight into the impact of classical gravitational fields on specific physical experiments [3]. Although these curvature effects predicted by general relativity are tremendous on cosmological scales, their influences in a laboratory on the earth are weak and difficult to detect. This is where the concept of analog models becomes relevant [4–7]. Analog models have gained prominence in physics and mathematics, offering new perspectives and enabling the exchange of ideas between different scientific disciplines [8]. In recent years, there have been numerous attempts to employ physical systems, as analogy platforms to simulate and explore some aspects of general relativity theory in laboratory [9–12]. For instance, analog models have been used to understand black hole physics, leading to the development of a thermodynamic theory for these objects and the discovery of the Hawking effect [13]. Furthermore, several types of analog physical systems on two-dimensional curved surfaces have been proposed to model the general relativity. Given a constant time and extracting the equatorial slice of Friedmann-Robertson-walker's space-time, we arrive at a two-dimensional curved surface with constant curvature. In these types of analog models, a curved space is created by engineering the geometry of the space itself to investigate its effects on certain physical systems [14, 15].

On the other hand, quantum thermodynamics [16, 17] has attracted considerable attention for elucidating the

fundamental relationship between quantum mechanics and thermodynamics [18]. The conversion of energy into mechanical work is essential for almost any industrial process [19]. Quantum thermodynamics investigates fundamental concepts such as temperature, heat, and work in the context of quantum physics. This field primarily focuses on studying thermal machines that operate in the quantum realm and determining how quantum properties can be exploited to enhance their efficiency. Quantum heat engines, which attracted much attention in recent year, are designed based on quantum thermodynamic cycles with different working substances, such as spin systems [20], single ions [21], harmonic-oscillators [22–24], quantum Brownian oscillators [25], two-level systems [26–28], single-particles [29–31], two-particles [32], multilevel systems [33, 34], optomechanical systems [35], and cavity quantum electrodynamics systems [36]. Among these, the so-called quantum Otto engine is presented which consists of a quantum working substance manipulated between two heat reservoirs under two adiabatic and two isochoric branches [37–39].

To address the question of the efficiency of a quantum heat engine, compared to its classical counterpart, several protocols have been proposed and analyzed [40]. In [41], it is shown that non-thermal baths, such as coherent bath [42] and squeezed bath [43], may impart not only heat, but also mechanical work to a heat engine. While such engines can exceed the Carnot efficiency, they do not violate the second-law of thermodynamics. Although the Carnot bound is inapplicable to such a hybrid machine, recent proposals suggest that a small scale heat engine may potentially exceed Carnot efficiency without requiring additional resources like coherence or correlations [44, 45].

In Ref. [46], by using a delta-coupled Unruh-Dewitt detector in Minkowski space-time, a relativistic quantum Otto engine is considered to extract work from a quantum field in a thermal state. The performance of a quantum Otto engine with a working medium of a relativistic

* s.kourkinejat@sci.ui.ac.ir

† a.mahdifar@sci.ui.ac.ir

‡ ehsan.amooghorban@sku.ac.ir

particle is analyzed in Ref.[47]. Additionally, the thermal properties of a quantum heat engine with a relativistic moving heat bath are investigated in Ref.[48]. In a related study, a quantum Otto engine was introduced, in which the effective temperatures observed by stationary moving observers are utilized [49]. Also, the amount of work extracted by an observer moving in a circular path is investigated in Ref.[50]. Further research has investigated how relativistic energies and space-time geometry affect the thermal efficiency of thermodynamic cycles [51]. However, the impact of curvature on the performance of quantum thermal engines remains a relatively unexplored topic.

In the present contribution, we adopt an analog model of general relativity to investigate the effects of spatial curvature on a quantum Otto engine. We consider a quantum Otto cycle with a quantum harmonic oscillator on a circle as its working substance. We assume that two classical hot and cold thermal baths are located at places with different curvatures. We calculate the curvature-dependent work and heat in our Otto cycle and study the curvature effects on its thermal efficiency. It is worth noting that the properties of the harmonic oscillator on a circle depend on the curvature of the circle, and therefore, making it a suitable platform to investigate the spatial curvature effects on this physical process. Moreover, this analog model has the advantage of being analytically tractable.

The paper is organized as follows. In Section II, we briefly review the quantum harmonic oscillator on a circle. In Section III, after a short review of the quantum Otto's engines, we propose our curvature-dependent scheme of a quantum Otto engine with a harmonic oscillator on a circle as the working substance. Section IV is devoted to investigating the efficiency of our engine, as well as its limiting case of small curvature (near the Earth surface) and large curvature (near massive celestial bodies like black holes). Then, equipped with the theoretical tools presented in previous sections, we present our results about the curvature effects on the efficiency of our quantum Otto's engine in Section V. Finally the summary and concluding remarks are given in Section VI.

II. QUANTUM HARMONIC OSCILLATOR ON CIRCLE

Quantum heat engines generate work by utilizing quantum systems as their working substance. To investigate the spatial curvature effects on a quantum Otto's engine, in this paper, we assume that the working substance is a quantum harmonic oscillator on a circle. Therefore, we begin with a brief introduction to the quantum harmonic oscillator on the circle.

Recently, some of the authors of this paper have studied the quantum dynamics of a harmonic oscillator constrained on a circle with radius R [52]. By using the

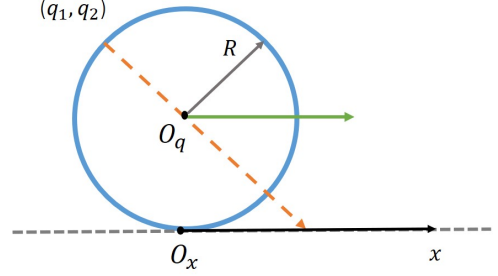


FIG. 1. Coordinate systems and the gnomonic projection from a circle with radius R onto a line.

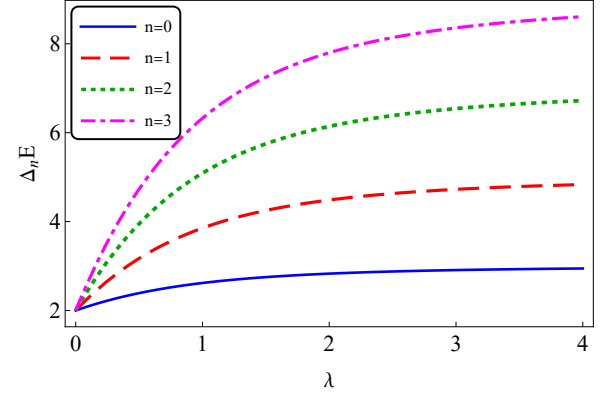


FIG. 2. Dimensionless energy gaps as a function of the spatial curvature parameter λ , for $n = 0, 1, 2, 3$.

gnomonic projection, which is a projection onto the tangent line from the center of the circle and denoting the Cartesian coordinate of this projection by x , we obtain the Hamiltonian of the quantum harmonic oscillator on a circle as follows:

$$\hat{H}(\lambda) = \frac{1}{2}[-(1+\lambda x^2)^2 \frac{d^2}{dx^2} - 2\lambda x(1+\lambda x^2) \frac{d}{dx}] + \frac{1}{2}x^2, \quad (1)$$

where $\lambda = 1/R^2$ is the curvature of the circle and the natural system of units is employed ($m = \hbar = \omega = 1$). The energy eigenvalues of the quantum oscillator on a circle are obtained as:

$$E_n(\lambda) = \gamma(n + \frac{1}{2}) + \frac{\lambda}{2}n^2, \quad (2)$$

where

$$\gamma = \frac{(\lambda + \sqrt{\lambda^2 + 4})}{2}. \quad (3)$$

As it is seen, the energy spectrum (2) is expressed as a function of the spatial curvature λ . It is obvious that in the limit of $\lambda \rightarrow 0$, γ approaches unity, and we recover the energy eigenvalues of the quantum harmonic oscillator on a straight line: $E_n(\lambda = 0) = (n + \frac{1}{2})$. It is worth noting that the spatial curvature parameter, which introduces a nonlinear character to the quantum oscillator on a circle, is reflected in the anharmonicity of the energy

spectrum. In other words, when we go from a flat line to a curved circle, the energy levels are no longer evenly spaced. Therefore, our quantum oscillator exhibits an effective piston-like behavior through variations of the curvature parameter λ .

In Fig. 2, we have plotted the dimensionless variation of energy gaps:

$$\Delta_n E(\lambda) = \frac{E_{n+1}(\lambda) - E_n(\lambda)}{E_0(\lambda)}, \quad (4)$$

as a function of the spatial curvature parameter. It is seen that for a fixed value of λ ($\lambda \neq 0$), the energy gaps increase with increasing the value of n . Furthermore, with increasing the curvature λ , the uniformity of the energy gaps between the eigen-energies is further lost.

III. QUANTUM CURVATURE-DEPENDENT OTTO ENGINE

In this section, we consider a quantum Otto's engine with a harmonic oscillator on a circle as its working substance, as illustrated in Fig. 3. This engine consists of two isochoric branches, one with a hot thermal bath and the other with a cold thermal bath at two different temperatures $T_h > T_c$ [53], [54]. A quantum isochoric process (constant volume process) is similar to its classical isochoric process. In contrast, a classical adiabatic thermodynamic process does not always require the occupation probabilities to remain constant, while a quantum adiabatic process proceeds slowly enough so that the generic quantum adiabatic condition is satisfied, and keeps the population distributions constant [55]. Moreover, during quantum adiabatic stages, the working substance Hamiltonian varies while population distribution remains constant [56]. It is worth mentioning that if this variation in the Hamiltonian causes the energy gaps to scale at a constant ratio, the efficiency of the engine is like its classical counterpart. However, if the deformation of the Hamiltonian leads to inhomogeneous energy gaps, the heat engine's efficiency can exceed its classical counterpart [57]. The first step in understanding the thermodynamics of a harmonic oscillator on a circle is to find the correct expression for the equilibrium distribution when the system is in contact with a thermal bath. The equilibrium distribution of a quantum oscillator on a circle, weakly coupled to a large classical bath, will eventually reach the corresponding Gibbs thermal equilibrium state, $\rho = \frac{e^{-\hat{H}(\lambda)/T}}{Z(\lambda)}$, [58] where the canonical partition function of the quantum oscillator, acting as the working substance of our Otto's engine, is given by

$$Z(\lambda) = \sum_n e^{-\frac{E_n(\lambda)}{T}}. \quad (5)$$

Here, we take k_B as unity and $E_n(\lambda)$ is given by (2).

It should be noted that in our analog model of the quantum Otto's cycle, we assume that the hot and cold thermal bath are located at two different heights above the

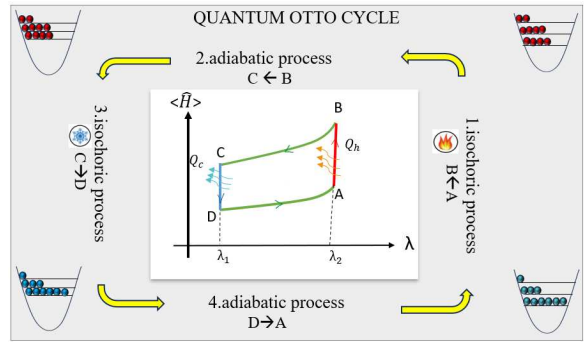


FIG. 3. An illustration of the mean energy-the spatial curvature, diagram of a quantum Otto cycle based on the harmonic oscillator on a circle

ground. In other words, to investigate the curvature effects of the physical space on the work done by the cycle, and the heat engine's efficiency, we place the hot thermal bath in a location with greater spatial curvature than the cold thermal bath, i.e. $\lambda_2 \geq \lambda_1$. However, we study these curvature effects using an analog model, presented by a quantum harmonic oscillator on a circle.

The internal energy is simply determined by the expectation value of the Hamiltonian over the state of the working substance as:

$$\langle \hat{H}(\lambda) \rangle = \sum_n P_n(\lambda) E_n(\lambda), \quad (6)$$

where the occupation probability of the system, $P_n(\lambda)$, in thermal equilibrium with the bath is given by

$$P_n(\lambda) = \frac{e^{-\frac{E_n(\lambda)}{T}}}{Z(\lambda)}. \quad (7)$$

A. Processes of a quantum Otto engine cycle

The quantum Otto cycle consists of four distinct stages [59]. In order to evaluate the performance of our quantum Otto's engine, we need to calculate the work and the heat during each stage. Heat is exchanged with the baths during the isochoric thermalization in the first and third stages, while work is performed during two and four unitary strokes [27].

1. Hot isochore ($A \rightarrow B$):

During step 1, the quantum working substance is connected to the heat bath at temperature T_h , converting from state A to B , with equal energy levels $E_n^B(\lambda_2) = E_n^A(\lambda_2)$. Moreover, the energy level gaps remain unchanged as the system absorbs energy, and the temperature of the working substance raises until it reaches thermal equilibrium with the hot bath. At the end of this isochoric process, the occupation probabilities in each eigenstate satisfies the Boltzmann distribution. Thus, the heat absorbed by the working substance from the

hot bath is given by:

$$Q_h = \sum_n E_n(\lambda) dP_n(\lambda) = \sum_n E_n^A(\lambda_2) [P_n^B(\lambda_2) - P_n^A(\lambda_2)]. \quad (8)$$

Furthermore, since the curvature is equal to λ_2 , no work is done during this step, and we have:

$$W_{A \rightarrow B} = 0.$$

2. Isentropic compression ($B \rightarrow C$):

After decoupling from the bath, the system undergoes a quantum adiabatic transformation from state B , with curvature λ_2 , to state C , with curvature λ_1 . In quantum adiabatic processes, the adiabatic condition is met when changes occur slowly enough to keep population distributions constant ($dP_n = 0$) and no heat is exchanged ($dQ = 0$). However, work can still be done during this process despite the lack of heat exchange. This transformation ensures that the probabilities in state C match those in state B , i.e., $P_n^C(\lambda_1) = P_n^B(\lambda_2)$, and the energy eigenvalues are adiabatically transferred from $E_n^B(\lambda_2) = E_n^A(\lambda_2)$ to $E_n^C(\lambda_1)$. Therefore, we have:

$$Q_{B \rightarrow C} = 0,$$

and

$$W_{B \rightarrow C} = \sum_n P_n dE_n = \sum_n P_n^B(\lambda_2) [E_n^A(\lambda_2) - E_n^C(\lambda_1)]. \quad (9)$$

3. Cold isochore ($C \rightarrow D$):

In the third step, the system cools down to point D , where the eigen-energy of the working substance remains the same as point C , i.e., $E_n^D(\lambda_1) = E_n^C(\lambda_1)$, while the population adjusts to $P_n^D(\lambda_1)$. The heat exchange between the substance and the cold bath, as well as the work done during the isochoric cooling can be calculated as:

$$Q_c = \sum_n E_n^C(\lambda_1) [P_n^D(\lambda_1) - P_n^C(\lambda_1)], \quad (10)$$

$$W_{C \rightarrow D} = 0.$$

4. Isentropic expansion ($D \rightarrow A$):

Ultimately, the system resets to its initial point A , by completing the cycle with another quantum adiabatic transformation, provided that $P_n^A(\lambda_2) = P_n^D(\lambda_1)$. In this adiabatic step, there is no heat exchange between the system and its surroundings, and the work can be directly determined by:

$$W_{D \rightarrow A} = \sum_n P_n^D(\lambda_2) [E_n^D(\lambda_2) - E_n^A(\lambda_1)]. \quad (11)$$

Also we have:

$$Q_{D \rightarrow A} = 0.$$

B. Work and heat of the quantum Otto cycle

Now we can obtain the net work performed by our quantum Otto engine [60] as follows:

$$\begin{aligned} W &= -(W_{C \rightarrow B} + W_{D \rightarrow A}) = Q_h - Q_c \quad (12) \\ &= \sum_n [E_n^A(\lambda_2) - E_n^C(\lambda_1)] [P_n^B(\lambda_2) - P_n^A(\lambda_2)]. \end{aligned}$$

It is worth noting that the factor $E_n^A(\lambda_2) - E_n^C(\lambda_1)$ represents the variation of the energy eigenvalue during quantum adiabatic transformations. We can evaluate work using the thermal population distribution $P_n^B(\lambda_2) = P_n^C(\lambda_1)$ and $P_n^D(\lambda_1) = P_n^A(\lambda_2)$. From this analysis, it should be evident that the quantum Otto's cycle is an irreversible process.

IV. THE THERMAL EFFICIENCY OF QUANTUM OTTO ENGINE

The first law of thermodynamics explains how to convert heat, which is a form of energy, into work. The second law tells how much of this heat can be converted into work. Efficiency is defined as the ratio of output energy to input energy [61]. The thermal efficiency of our Otto cycle is defined by

$$\eta = \frac{W}{Q_h}, \quad (13)$$

where the heat injected into the system from the hot bath, Q_h , is given by equation (8).

A. LIMITING CASE OF THERMAL EFFICIENCY

In this section, we consider two limiting cases of our curvature-dependent Otto engine's thermal efficiency (13): the small spatial curvature limit and the large spatial curvature limit. In these limiting cases, we assume that the curvature difference between the position of the cold and the hot bath, denoted by ε is too small, so that $\lambda_1 = \lambda - \varepsilon$ and $\lambda_2 = \lambda$.

1. The small spatial curvature limit:

Here, we calculate the efficiency in the small spatial curvature limit, such as, near the Earth, assuming a slight difference in spatial curvatures and a small temperature difference between the two heat sources. Defining the temperature difference between two baths as ($\theta = T_h - T_c$), and expressing the temperature of the hot bath in terms of the cold bath by $\frac{1}{T_h} = \frac{1}{T_c} - \frac{\theta}{T_c^2}$, we can then write

$$W \simeq \frac{\varepsilon \theta}{Z_A(\lambda) T_A^2} \sum_{n=0}^{\infty} E'_n(\lambda) E_n(\lambda) e^{-\frac{E_n(\lambda)}{T_A}}, \quad (14)$$

and

$$Q_h \simeq \frac{\theta}{Z_A(\lambda)T_A^2} \sum_{n=0}^{\infty} E_n^2(\lambda) e^{-\frac{E_n(\lambda)}{T_A}}. \quad (15)$$

Here, we assume that, in this limiting case, $Z_A(\lambda) \simeq Z_B(\lambda)$, and $E'_n(\lambda)$ refers to the derivative of Eq.(2) with respect to λ . For small value of λ , this derivative is approximately equal to $(n^2 + n + \frac{1}{2})/2$. Now, by using these approximate relations, the following compact form is obtained for our engine's efficiency:

$$\eta_s \simeq \frac{\varepsilon E'_0}{E_0} \left(1 + \frac{E_1 E'_1}{E_0 E'_0} e^{-\frac{E_1 - E_0}{T_A}}\right). \quad (16)$$

For small curvature differences, such as $\lambda_2 = 0.011$, $\lambda_1 = 0.01$ and $\theta = 0.05$, the engine's approximate efficiency $\eta_s \simeq 0.001488$ closely matches the exact value from Eq.(13): $\eta = 0.001314$. It turns out that the two values are in near agreement.

2. The large spatial curvature limit:

To investigate thermal efficiency when the spatial curvature takes on its most extreme possible values, such as near a super massive black holes, we assume in our analog model that two values of λ_1 and λ_2 , are nearly large, but their difference remains small. Therefore, the change in eigenstate energies can be written as:

$$\Delta E_n = E_n^A(\lambda) - E_n^C(\lambda - \varepsilon) \cong (n+1)^2. \quad (17)$$

Considering that λ approaches large values, it can be easily shown that $\gamma \simeq \lambda$. To carry out our study, we need the Jacobi theta function to calculate the expansion coefficients, which is defined as [62]:

$$\vartheta_3(z, q) = 1 + 2 \sum_{n=1}^{\infty} q^{n^2} \cos(2nz). \quad (18)$$

By choosing $z = 0$ and $q = e^{-\frac{\lambda}{2T}}$, the following relations hold:

$$\sum_{n=0}^{\infty} q^{(n+1)^2} = \frac{\vartheta_3(q) - 1}{2}, \quad (19)$$

$$\sum_{n=0}^{\infty} (n+1)^2 q^{(n+1)^2} = \frac{q}{2} \vartheta'_3(q), \quad (20)$$

where the prime indicates a derivative with respect to its argument. Using Eq. (19) and (20), the harvested work and the heat absorbed during our quantum heat engine cycle are respectively, written as

$$W = \frac{\varepsilon}{2} \left[\frac{q_h \theta'_3(q_h)}{\theta_3(q_h) - 1} - \frac{q_c \theta'_3(q_c)}{\theta_3(q_c) - 1} \right],$$

$$Q_h = \frac{\lambda}{2} \left[\frac{q_h \theta'_3(q_h)}{\theta_3(q_h) - 1} - \frac{q_c \theta'_3(q_c)}{\theta_3(q_c) - 1} \right],$$

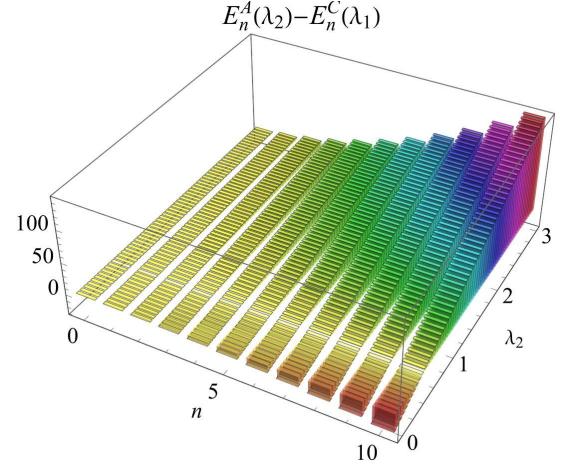


FIG. 4. $E_n^A(\lambda_2) - E_n^C(\lambda_1)$ during the adiabatic transformations versus n and λ_2 for $T_h = 1$ and $T_c = 0.1$.

where $q_h = e^{-\frac{\lambda}{2T_h}}$ and $q_c = e^{-\frac{\lambda}{2T_c}}$. Bearing these in mind, it is easily seen that the efficiency of our quantum heat engine, up to the leading order of ε , is given by:

$$\eta_l \simeq \frac{\varepsilon}{\lambda}. \quad (21)$$

For example, if we set $\lambda_1 = 9.8$ and $\lambda_2 = 10$, the approximate efficiency of the engine, i.e., $\eta_l = \frac{\varepsilon}{\lambda} = 0.02$, is very close to the exact value of $\eta = 0.0197$. In this limiting case, we see that the engine's efficiency is independent of temperature.

V. RESULTS AND REMARKS

In this section, we proceed to study the effects of curvature on our quantum Otto's engine using the analog model of a simple quantum harmonic oscillator on a circle. As shown in Eq. (12), the work extracted and thus the heat engine's efficiency of our proposed quantum Otto's heat engine depend on the net variation of the energy eigenvalues between points A and C , as well as the population difference between points A and B . More precisely, during the quantum Otto's cycle, the curvature of space changes from λ_2 to λ_1 , the structure of the energy levels varies from $E_n^A(\lambda_2)$ to $E_n^C(\lambda_1)$ and as a result, the distance between the energy levels gaps, $E_n^A(\lambda_2) - E_n^C(\lambda_1)$, changes. In contrast, during the quantum isentropic process in the stage 1, the interaction of the system with the heat source changes, the population differences, $P_n^B(\lambda_2) - P_n^A(\lambda_2)$. As is evident, these changes depend on the curvature of space.

In Fig. 4, we have plotted the variation of energy eigenvalue, $E_n^A(\lambda_2) - E_n^C(\lambda_1)$, versus λ_2 and n for $\lambda_1 = 0.5$. It is seen that the variation of energy eigenvalues between the point A (with the curvature λ_2) and the point C (with the curvature λ_1) increases with enhancement of

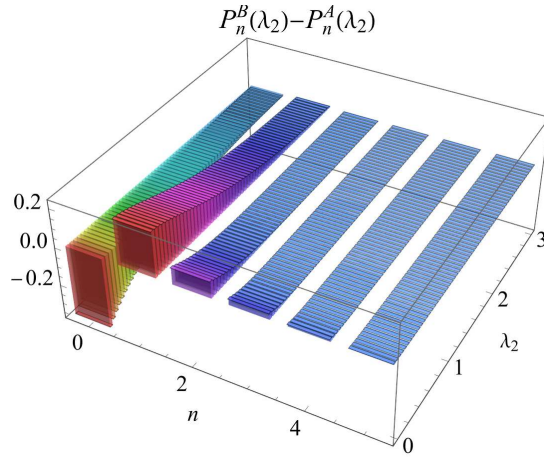


FIG. 5. $P_n^B(\lambda_2) - P_n^A(\lambda_2)$ versus n and λ_2 for $T_h = 1$ and $T_c = 0.1$.

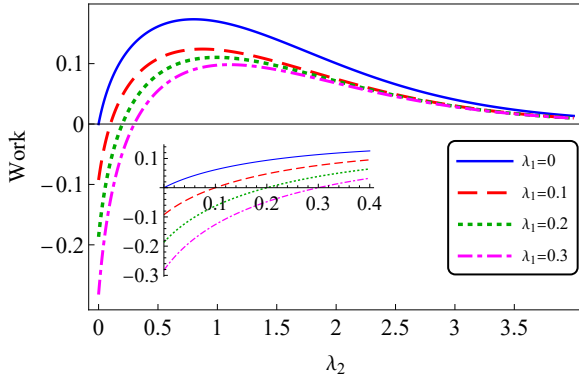


FIG. 6. Extracted work versus the spatial curvature of the working substance λ_2 for $(T_h = 1)$ and $(T_c = 0.1)$.

n . Moreover, $E_n^A(\lambda_2) - E_n^C(\lambda_1)$ is negative when $\lambda_2 < \lambda_1$, zero when $\lambda_2 = \lambda_1$, and positive when $\lambda_2 > \lambda_1$.

In Fig. 5, we display the population differences, $P_n^B(\lambda_2) - P_n^A(\lambda_2)$, as functions of λ_2 and n for the hot bath temperature $T_h = 1$ and the cold bath temperature $T_c = 0.1$. As is seen, the population differences decrease with increasing the value of n and also increasing the curvature of space λ_2 . This indicates that from A to B , the population differences for a fixed value of n are greater in flat space than in curved space.

Fig. 6 displays the total work extracted from the quantum Otto engine as a function of the spatial curvature λ_2 in which the hot bath is located, for several values of the curvature of the cold bath location, with $T_h = 1$ and $T_c = 0.1$.

A fundamental condition for the performance of a heat engine is the positive work extraction: $W_{ext} \geq 0$. The inset of Fig. 6 clearly illustrates that, the positive work can be extracted from our quantum Otto engine, provided that: $\lambda_2 > \lambda_1$. When there is no change in the curvature of space, i.e., $\lambda_2 = \lambda_1$, there is also no change in the energy eigenvalues between A and C and the work

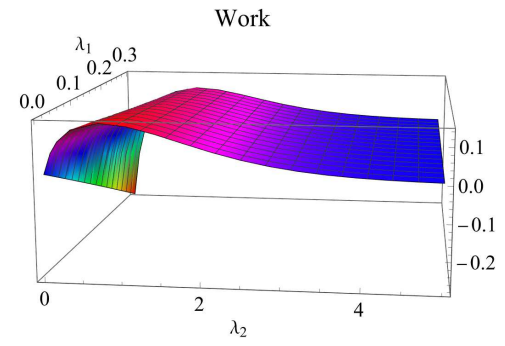


FIG. 7. The extracted work versus the spatial curvatures λ_1 and λ_2 for $T_h = 1$ and $T_c = 0.1$.

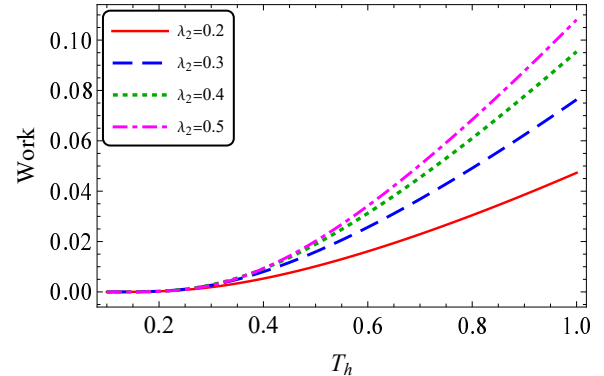


FIG. 8. The extracted work versus hot bath temperatures, T_h , for $T_c = 0.1$ and $\lambda_1 = 0.1$.

extracted from the quantum Otto machine is zero. Also, when $\lambda_2 < \lambda_1$, the extracted work becomes negative. This shows the motivation behind our initial assumption of placing the hot reservoir in a more curved space than the cold reservoir.

It should be noted that by choosing $\lambda_2 > \lambda_1$, the total extracted work first increases with the increase of λ_2 and then tends to zero. In addition, it is seen that the extracted work decreases with the increase of the curvature λ_1 . Also, the peaks shift toward larger value of λ_2 as λ_1 increases.

In order to illustrate obtained results more clearly, in Fig. 7 we have also displayed a three-dimensional plot of the extracted work versus the curvatures λ_1 and λ_2 .

In Fig. 8, the extracted work is plotted versus T_h for different values of λ_2 for $T_c = 0.1$ and $\lambda_1 = 0.1$. The results clearly show that for a fixed value of λ_2 , the extracted work is increased with increasing the temperature difference between the hot and the cold bath. On the other hand, for a given temperature T_h , increasing the curvature λ_2 leads to an increase in the extracted work. In other words, the increase in the difference between the curvatures λ_1 and λ_2 (the height of the hot bath and cold bath) plays a compensation role against the decrease in the difference between the temperature T_h and T_c .

In Fig. 9, we have plotted the heat engine's efficiency

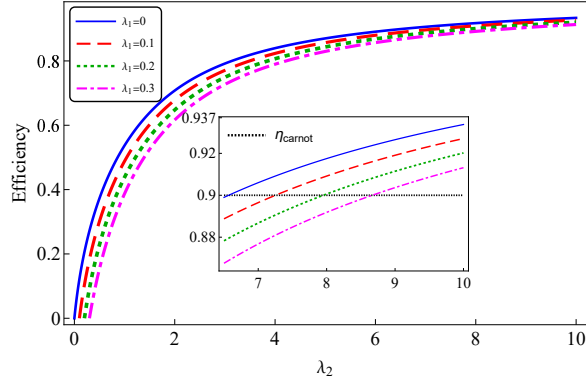


FIG. 9. The quantum Otto engine's efficiency as a function of λ_1 and λ_2 for hot and cold bath temperatures $T_h = 1$ and $T_c = 0.1$, respectively.

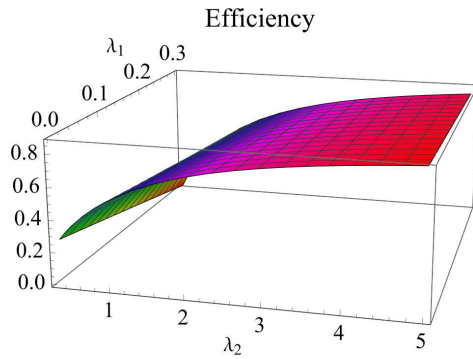


FIG. 10. The efficiency of quantum Otto cycle versus λ_1 and λ_2 for $T_h = 1$ and $T_c = 0.1$

versus the spatial curvature, λ_2 for $T_h = 1$, $T_c = 0.1$ and different values of λ_1 . This figure clearly show that for any fixed value of λ_1 , increasing spatial curvature of the hot bath location λ_2 , leads to a rapid increase in the heat engine's efficiency until it reaches a stable value.

One of the important factors in enhancing the efficiency of a quantum heat engine over its classical counterpart is that the change in the Hamiltonian of it's working substance should be such that the difference between the energy gaps during the engine's irreversible process changes in an anharmonicity manner [57].

It is worth noting that the results of Fig. 9 indicate that the efficiency of our analog heat engine model depends on the spatial curvature of the working substance's location. Therefore, by utilizing a quantum harmonic oscillator on a circle as the working substance, we can con-

trol the work and efficiency of the Otto engine. Moreover, it is possible to enhance it's efficiency to an upper limit that is greater than the Carnot efficiency bound ($\eta_{Carnot} = 1 - \frac{T_{cold}}{T_{hot}}$), by adjusting the curvature of space parameters λ_1 and λ_2 (the height of the hot and cold baths). The inset of Fig. 9 clearly shows that the efficiency of our Otto engine exceeds the Carnot efficiency limit.

On the other hand, for any fixed value of λ_2 , increasing the value of λ_1 and thus, decreasing the distance between hot and cold baths, leads to a decrease in heat engine's efficiency. A similar result is also observed in a quantum Otto heat engine with a relativistically moving thermal bath. When the hot bath moves at a relativistic speed relative to the cold bath, the distance between the two sources contracts, and thus, the heat engine is less efficient [63].

Finally, to better visualize the results that have been obtained, we display in Fig. 10 the variation of our engine efficiency versus the curvatures λ_1 and λ_2 .

VI. SUMMARY AND CONCLUDING REMARKS

In this paper, we have considered a quantum Otto's engine with a quantum harmonic oscillator on a circle as it's working substance, serving as an analog model of general relativity. By utilizing the curvature-dependent energies of this oscillator, we have investigated how the curvature effects of the physical space affects the properties of our quantum heat engine. Assuming that two thermal baths are located at places with different curvatures, we have calculated the curvature-dependent work and heat, with a particular focus on the effects of curvature on it's thermal efficiency. The result show that by adjusting the curvature difference between the bath's locations, we can control the efficiency of our heat engine, potentially allowing it to exceed the Carnot efficiency limit.

ACKNOWLEDGMENTS

We gratefully acknowledge support for this work by the Office of Graduate Studies and Research of Isfahan for their support. We would also like to extend our thanks to Shahrekord University for their assistance.

[1] V. H. Schultheiss, S. Batz, and U. Peschel, Nat. Photon. **10**, 106 (2016).
[2] S. Akbari-Kourbolagh, A. Mahdifar, and H. Mohammadi, arXiv:2406.12481 (2024).
[3] A. Mahdifar, M. J. Farsani, and M. B. Harouni, J. Opt. Soc. Am. B **30**, 2952 (2013).
[4] M. Rego-Monteiro, Eur. Phys. J. C **21**, 749 (2001).
[5] C. Xu and L.-G. Wang, Photon. Res. **9**, 2486 (2021).

[6] R. Bekenstein, J. Nemirovsky, I. Kaminer, and M. Segev, Phys. Rev. X **4**, 011038 (2014).

[7] C. Xu, A. Abbas, L.-G. Wang, S.-Y. Zhu, and M. S. Zubairy, Phys. Rev. A **97**, 063827 (2018).

[8] S. Dehdashti, R. Roknizadeh, and A. Mahdifar, J.Mod.Opt **60**, 233 (2013).

[9] C. Xu, A. Abbas, and L.-G. Wang, Opt. Express **26**, 33263 (2018).

[10] V. H. Schultheiss, S. Batz, and U. Peschel, Nat. Photon. **10**, 106 (2016).

[11] A. Mahdifar, S. Dehdashti, R. Roknizadeh, and H. Chen, Quantum Inf. Process **14**, 2895 (2015).

[12] A. Mahdifar, W. Vogel, T. Richter, R. Roknizadeh, and M. H. Naderi, Phys. Rev. A **78**, 063814 (2008).

[13] C. R. Almeida and M. J. Jacquet, EPJ H **48**, 15 (2023).

[14] S. B. Vincent H. Schultheiss and U. Peschel, ADV PHYS-X **5**, 1759451 (2020).

[15] W. Ding and Z. Wang, J. Opt **23**, 095603 (2021).

[16] F. Binder, L. A. Correa, C. Gogolin, J. Anders, and G. Adesso, *Thermodynamics in the Quantum Regime* (Springer Cham, 2018).

[17] P. Strasberg, G. Schaller, T. Brandes, and M. Esposito, Phys. Rev. X **7**, 021003 (2017).

[18] S. Chand and A. Biswas, Phys. Rev. E **95**, 032111 (2017).

[19] V. Blickle and C. Bechinger, Nat. Phys **8**, 143 (2012).

[20] X. Liu, L. Chen, F. Wu, and F. Sun, J.JOEI **87**, 69 (2014).

[21] S. Chand and A. Biswas, EPL **118**, 60003 (2017).

[22] H. T. Quan, Phys. Rev. E **79**, 041129 (2009).

[23] J. Wang, Z. Ye, Y. Lai, W. Li, and J. He, Phys. Rev. E **91**, 062134 (2015).

[24] P. Chattopadhyay, T. Pandit, A. Mitra, and G. Paul, J. Phys. A **584**, 126365 (2021).

[25] G. S. Agarwal and S. Chaturvedi, Phys. Rev. E **88**, 012130 (2013).

[26] V. Mehta and R. S. Johal, Phys. Rev. E **96**, 032110 (2017).

[27] G. Jiao, S. Zhu, J. He, Y. Ma, and J. Wang, Phys. Rev. E **103**, 032130 (2021).

[28] J. Wang, Z. Wu, and J. He, Phys. Rev. E **85**, 041148 (2012).

[29] M. Beau, J. Jaramillo, and A. Del Campo, Entropy **18** (2016).

[30] J. P. S. Peterson, T. B. Batalhão, M. Herrera, A. M. Souza, R. S. Sarthour, I. S. Oliveira, and R. M. Serra, Phys. Rev. Lett. **123**, 240601 (2019).

[31] D. Gelbwaser-Klimovsky, A. Bylinskii, D. Gangloff, R. Islam, A. Aspuru-Guzik, and V. Vuletic, PRL **120**, 170601 (2018).

[32] M. Boubakour, T. Fogarty, and T. Busch, Phys. Rev. Res. **5**, 013088 (2023).

[33] H. T. Quan, P. Zhang, and C. P. Sun, Phys. Rev. E **72**, 056110 (2005).

[34] R. Uzdin and R. Kosloff, New J. Phys **16**, 095003 (2014).

[35] K. Zhang, F. Bariani, and P. Meystre, Phys. Rev. A **90**, 023819 (2014).

[36] J. Wang, J. He, and X. He, Phys. Rev. E **84**, 041127 (2011).

[37] G. Thomas and R. S. Johal, Phys. Rev. E **83**, 031135 (2011).

[38] T. D. Kieu, Eur. Phys. J. D **39**, 115 (2006).

[39] R. Kosloff and Y. Rezek, Entropy **19** (2017).

[40] N. H. Y. Ng, M. P. Woods, and S. Wehner, New J. Phys **19**, 113005 (2017).

[41] W. Niedenzu, D. Gelbwaser-Klimovsky, A. G. Kofman, and G. Kurizki, New J. Phys **18**, 083012 (2016).

[42] M. O. Scully, K. R. Chapin, K. E. Dorfman, M. B. Kim, and A. Svidzinsky, PNAS **108**, 15097 (2011).

[43] J. Roßnagel, O. Abah, F. Schmidt-Kaler, K. Singer, and E. Lutz, Phys. Rev. Lett. **112**, 030602 (2014).

[44] M. O. Scully, Phys. Rev. Lett. **104**, 207701 (2010).

[45] A. Levy and D. Gelbwaser-Klimovsky, Quantum features and signatures of quantum thermal machines, in *Thermodynamics in the Quantum Regime: Fundamental Aspects and Applications*, edited by F. Binder, L. A. Correa, C. Gogolin, J. Anders, and G. Adesso (Springer International Publishing, Cham, 2018) pp. 87–126.

[46] N. K. Kollas and D. Moustos, Phys. Rev. D **109**, 065025 (2024).

[47] N. M. Myers, O. Abah, and S. Deffner, New J. Phys **23**, 105001 (2021).

[48] N. Papadatos, Int. J. Theor. Phys **60**, 4210 (2021).

[49] M. Good, B. A. Juárez-Aubry, D. Moustos, and M. Temirkhan, JHEP **2020** (6), 1.

[50] K. Gallock-Yoshimura, V. Thakur, and R. B. Mann, Front. Phys **11**, 1287860 (2023).

[51] N. M. Myers, O. Abah, and S. Deffner, New J. Phys **23**, 105001 (2021).

[52] A. Mahdifar and E. Amooghorban, Int. J. Geom. Meth. Mod. Phys. **19**, 2250140 (2022).

[53] B. Leggio and M. Antezza, Phys. Rev. E **93**, 022122 (2016).

[54] J.-F. Chen, C.-P. Sun, and H. Dong, Phys. Rev. E **100**, 032144 (2019).

[55] H. T. Quan, Y.-x. Liu, C. P. Sun, and F. Nori, Phys. Rev. E **76**, 031105 (2007).

[56] F. Ozaydin, O. E. Müstecaplıoğlu, and T. b. u. Hakioglu, Phys. Rev. E **108**, 054103 (2023).

[57] D. Gelbwaser-Klimovsky, A. Bylinskii, D. Gangloff, R. Islam, A. Aspuru-Guzik, and V. Vuletic, Phys. Rev. Lett. **120**, 170601 (2018).

[58] S. Deffner and S. Campbell, *Quantum Thermodynamics: An introduction to the thermodynamics of quantum information* (Morgan & Claypool Publishers, 2019).

[59] Z. Fei, J.-F. Chen, and Y.-H. Ma, Phys. Rev. A **105**, 022609 (2022).

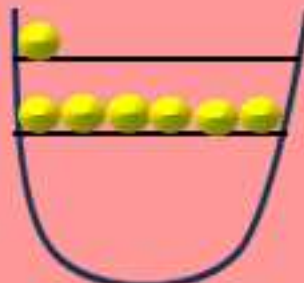
[60] M. F. Anka, T. R. de Oliveira, and D. Jonathan, Phys. Rev. E **104**, 054128 (2021).

[61] O. Abah and E. Lutz, EPL **118**, 40005 (2017).

[62] E. W. Weisstein, <https://mathworld.wolfram.com/> (2000).

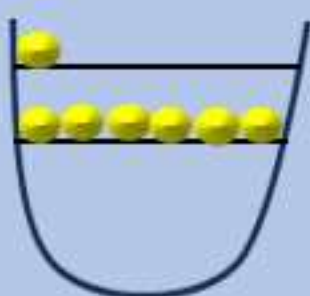
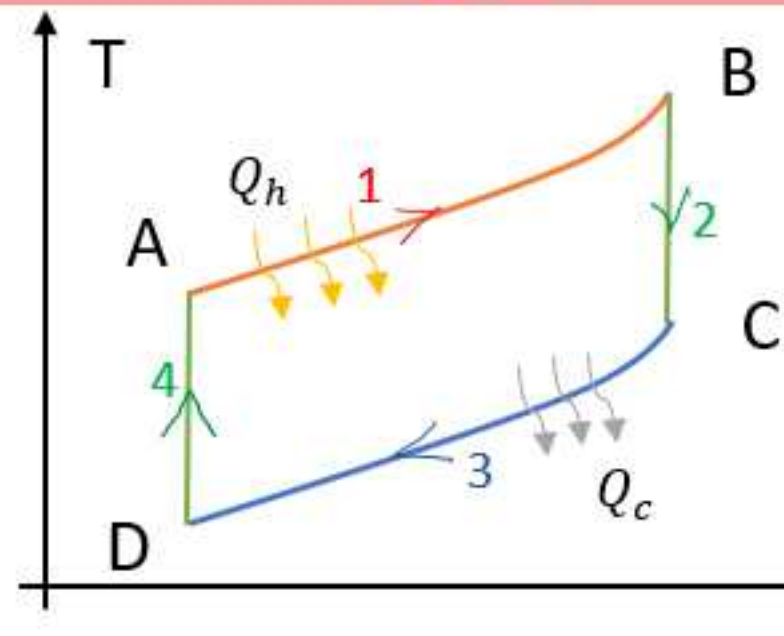
[63] N. Papadatos, Int. J. Theor. Phys **60**, 4210 (2021).

QUANTUM OTTO CYC



1. isochoric process
 $A \rightarrow B$

4. adiabatic process
 $A \leftarrow D$



3. isochoric process
 $D \leftarrow C$

$$\lambda_A > \lambda_C$$

